DOI: 10.1002/ejic.200500751

N–H···S Hydrogen Bonds in a New Family of Ion-Pair Complexes Between Cationic Nickel Tetraazabicyclononane and Anionic Metal Dithiolates: Synthesis, Characterization and Properties of $[Ni(C_9H_{22}N_6)][M(mnt)_2]$ (M^{II} = Cu, Ni, Pd)

Vedichi Madhu[a] and Samar K. Das*[a]

Keywords: Hydrogen bonds / Ion pairs / N ligands / Nickel / S ligands

The ion-pair complexes $[Ni(C_9H_{22}N_6)][Cu(mnt)_2]$ (**1**), $[Ni(C_9H_{22}N_6)][Ni(mnt)_2]$ (**2**), and $[Ni(C_9H_{22}N_6)][Pd(mnt)_2]$ (**3**; mnt^{2-} = 1,2-dicyanoethylenedithiolate, $C_9H_{22}N_6$ = 3,7-bis(2-aminoethyl)-1,3,5,7-tetraazabicyclo[3.3.1]nonane) have been synthesized and characterized by elemental analysis, IR, UV/Vis, and ^1H NMR spectroscopy, X-ray powder diffraction, and electrochemical studies, and unambiguously by single-crystal X-ray crystallography. All three complexes are isostructural and crystallize in the monoclinic space group $P2_1/n$. The N–H···S-type hydrogen-bonding capabilities of the classical sulfur-containing complex anions $[M^{II}(mnt)_2]^{2-}$ (A; M = Cu, Ni and Pd) have been explored using amine groups containing the nickel complex cation $[Ni(C_9H_{22}N_6)]^{2+}$ (C) in the ion-pair compounds **1**, **2**, and **3**. In the crystal, the cation interacts with two different anions through three N–H···S hydrogen bonds and, likewise, the anion is hydrogen-bonded to two different cations through three hydrogen bonds, resulting in the formation of a chain-like arrangement. The average N–H···S hydrogen-bond lengths are 3.498(3), 3.505(3), and 3.490(5) Å for compounds **1**, **2**, and **3**, respectively. Another crystallographic feature is the presence of CC–AA–CC–AA-type packing with short S···Ni contacts in the crystal structures. Besides crystallography, the existence of these N–H···S hydrogen bonds between cation $[Ni(C_9H_{22}N_6)]^{2+}$ (C) and anion $[M^{II}(mnt)_2]^{2-}$ (A) is strongly supported by the IR and ^1H NMR studies. The stability of the $[Ni(C_9H_{22}N_6)]^{2+}$ (C) moiety in compounds **1**, **2**, and **3** is discussed in light of electrochemical studies performed on these compounds and $[Ni(C_9H_{22}N_6)](ClO_4)_2$. Complex **1** exhibits a well-resolved ESR signal corresponding to a Cu^{2+} (d^9) system at liquid-nitrogen temperature.

Introduction

The assembly of cationic and anionic components into ion-pair-containing supramolecular systems in which the positive and negative partners interact through noncovalent hydrogen bonding and/or π–π interactions is a challenging task in modern chemistry.[1] Bis(1,2-dithiolene)–transition metal complexes have been extensively studied as one of the ion-pair components because of their importance as functional materials, for example as near-infrared (NIR) laser dyes,[2] conducting[3] and magnetic materials,[4] and in nonlinear optics.[5] The molecular-conductor-type ion-pair charge-transfer (IPCT) complexes $[A^{2+}\{ML_2\}^{2-}]$ [A^{2+} = bipyridinium dication derivative, $[ML]^{2-}$ = metal bis(dithiolate), M^{2+} = Ni, Pd, Pt, and Cu] exhibit an IPCT transition in the solid state due to a supramolecular electronic interaction between the cation and anion.[6] A class of ion-pair complexes has been obtained with a combination of uncharged organic components and, in this case, the ion pairing is achieved by a radical mechanism.[7] Although charge-transfer (CT) complexes of metal dithiolenes with organic cations as acceptors have been investigated quite well, including their structural characterization, ion-pair complexes of metal dithiolenes with transition metal inorganic complexes as cations are rare.[8] We have been working on ion-pair supramolecular systems in order to explore the noncovalent, hydrogen-bonding interactions between cationic and anionic components by choosing appropriate H-bond donor and acceptor sites. We have recently reported the NIR absorption due to a supramolecular electronic interaction between an anion and cation in a three-dimensional hydrogen-bonded networking material, namely [4,4′-H_2bpy][$Cu(mnt)_2$], emphasizing the N–H···N-type hydrogen bonding between cation and anion.[9] Now we extend this study to an inorganic transition metal complex, NiL^{2+} {L = $C_9H_{22}N_6$ = 3,7-bis(2-aminoethyl)-1,3,5,7-tetraazabiclo[3.3.1]nonane} as a cation and $[M^{II}(mnt)_2]^{2-}$ (M = Cu, Ni and Pd; mnt^{2-} = 1,2-dicyanoethylenedithiolate) as anions in ion-pair complexes (Scheme 1).

[a] School of Chemistry, University of Hyderabad, Hyderabad 500 046, India
Fax: +91-40-2301-2460
E-mail: skdsc@uohyd.ernet.in

Supporting information for this article is available on the WWW under http://www.eurjic.org or from the author.

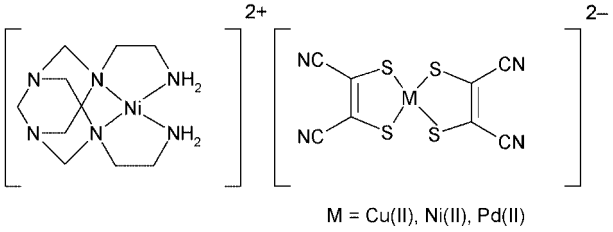

Scheme 1.

In this group of ion-pair complexes the nickel complex cation has coordinated NH_2 groups. The aim of this work was to examine whether these amine hydrogens form N–H···S-type hydrogen bonds with the thiolate sulfur of the mnt ligands of the anions. Living systems contain several important sulfur-containing molecules, such as cysteine and methionine, and hydrogen bonding between amide groups and the cysteine sulfur is a common feature of all iron-sulfur proteins.[10] For example, the formation of N–H···S hydrogen bonds plays a crucial role in the function of many proteins, including *Pasteurella aerogenes* ferredoxin and *Clostridium pasteurianum* rubredoxin.[11] Much of the importance of the N–H···S hydrogen-bonding interaction derives from the fact that it may modulate the redox potentials of several of these proteins.[10,12] Therefore, the study of N–H···S hydrogen bonds using simple inorganic compounds may have fundamental importance in understanding the chemical functions of those metal-associated proteins in which the negative metal–sulfur cluster is hydrogen-bonded to the surrounding amide groups of peptides/proteins. Various metal thiolate complexes have been synthesized and structurally characterized as model compounds of these natural proteins.[13] In many of these model studies, intramolecular N–H···S hydrogen-bonding interactions are observed because the ligand coordinated to the metal center has amide-type functional groups. Intermolecular amide–thiolate hydrogen-bonding interactions have been described[14] for the complex $[(CH_3)_3NCH_2CONH_2]_2[Co(SC_6H_5)_4]$ and the metal-free compound $[(CH_3)_3NCH_2CONH_2][SC_6H_5]$. Herein we describe the synthesis, crystal structures, and properties of a new family of ion-pair complexes, namely $[Ni(C_9H_{22}N_6)][Cu(mnt)_2]$ (**1**), $[Ni(C_9H_{22}N_6)][Ni(mnt)_2]$ (**2**), and $[Ni(C_9H_{22}N_6)][Pd(mnt)_2]$ (**3**), all of which contain N–H···S hydrogen bonds between the cation and anion in their ion pairs. Our results show a systematic decrease in $M–S_H$ bond lengths with respect to the $M–S_N$ bond length ($M = Cu^{2+}$, Ni^{2+} and Pd^{2+}; S_H is the sulfur atom involved in hydrogen bonding and S_N that which is not involved in hydrogen bonding). We explain this trend in terms of N–H···S hydrogen-bonding interactions. We also describe detailed IR and ^1H NMR studies that support the existence of N–H···S hydrogen bonds between the cation (C) and anion (A).

Results and Discussion

Synthesis

The reaction of $[Ni^{II}(C_9H_{22}N_6)](ClO_4)_2$ with $[Bu_4N]_2[M^{II}(mnt)_2]$ (M = Cu, Ni, and Pd) in MeCN solution leads to the isolation of the ion-pair complexes $[Ni(C_9H_{22}N_6)][M(mnt)_2]$. The relevant reactions can be described according to Equation (1).

$$[Ni^{II}(C_9H_{22}N_6)](ClO_4)_2 + [Bu_4N]_2[M^{II}(mnt)_2] \rightarrow [Ni^{II}(C_9H_{22}N_6)][M^{II}(mnt)_2] + 2\,Bu_4NClO_4 \quad (1)$$

Crystals of compounds **1** (M = Cu), **2** (M = Ni), and **3** (M = Pd) gave satisfactory elemental analyses. The numbers of Cu and Ni sites in compound **1** and of Pd and Ni sites in compound **3**, as revealed by single-crystal X-ray structure analyses, are consistent with the results of EDAX analyses, which gave an average Ni/Cu value of around 1:1 for compound **1** and a Ni/Pd value of about 1:1 for compound **3**. All three compounds were obtained in high yield. However, these high-yield procedures produced microcrystalline products instead of the single crystals required for crystal-structure determination. Single crystals were obtained by a slow-diffusion technique, as described in the Experimental Section.

X-ray Powder-Diffraction Studies

X-ray powder-diffraction patterns of microcrystalline compounds **1**–**3** were recorded. The simulated patterns were generated from the single-crystal X-ray data of the appropriate compounds obtained by the slow-diffusion technique. The simulated patterns match the respective experimentally observed powder-diffraction patterns very well, as shown in SI-Figure 38 (see Supporting Information). This confirms the homogeneity and the purity of the bulk samples **1**–**3**.

Description of the Structures

Complexes **1**–**3** crystallize in the monoclinic space group $P2_1/n$. A thermal ellipsoidal plot of the non-hydrogen atoms is presented in Figure 1. This shows the presence of $[Ni(C_9H_{22}N_6)]^{2+}$ as a cation and $[M(mnt)_2]^{2-}$ as an anion. The four nitrogen donor atoms in the $[Ni(C_9H_{22}N_6)]^{2+}$ cation form a plane with a maximum deviation of 0.0022 Å. The nickel ion is displaced by 0.040(1) Å from the least-squares plane. The average Ni–N bond length is 1.913 ± 0.002 Å, which is about 0.01 Å longer than those in the crystal structure of the previously reported[15] compound $[Ni(C_9H_{22}N_6)](ClO_4)_2$, which contains the same cation. However, the quality of the crystal of this complex was too poor to be refined aniosotropically (disorder problem of the whole cation in addition to disordered perchlorate anions).[15] This is reflected in some of the C–N bond lengths, which are either unreasonably short or unreasonably long. In the present study, we were able to overcome this disorder problem of the $[Ni(C_9H_{22}N_6)]^{2+}$ cations in complexes **1**–**3**. There are 14 N–C single bonds in the ligand $C_9H_{22}N_6$ (Figure 1). Depending on the environments of the nitrogen atoms in the $[Ni(C_9H_{22}N_6)]^{2+}$ cation, the N–C bond lengths show systematic variations ranging from 1.433 to 1.522 Å for compound **1**. There are four tertiary nitrogen atoms, namely N(7), N(8), N(9), and N(10). The six bonds

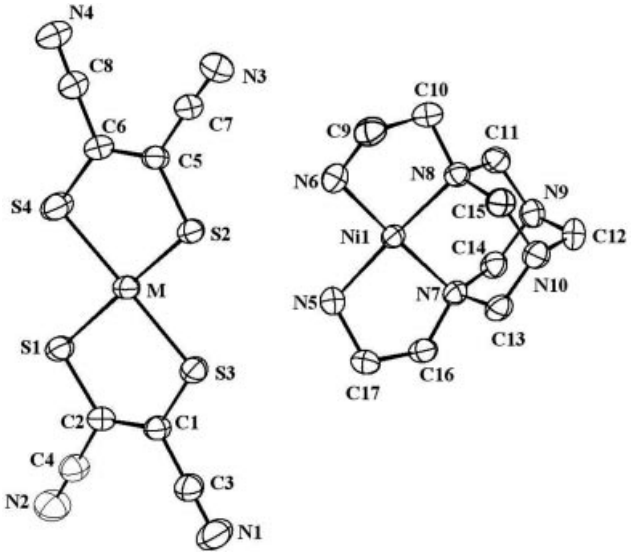

Figure 1. Thermal ellipsoidal plot (50% probability) of compounds $[Ni(C_9H_{22}N_6)][M(mnt)_2]$ (M = Cu^{2+}, Ni^{2+} and Pd^{2+}). Hydrogen atoms have been omitted for clarity.

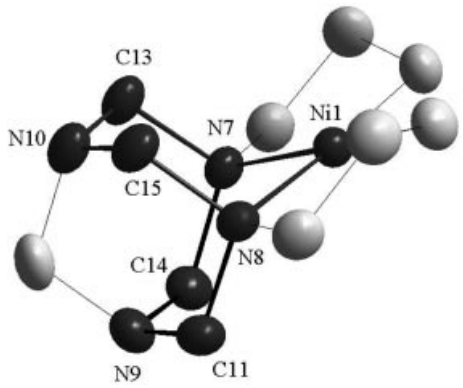

Figure 2. The molecular structure of $[Ni(C_9H_{22}N_6)]^{2+}$ in **1**–**3** showing the chair form of the six-membered chelate ring [Ni(1)–N(7)–C(14)–N(9)–C(11)–N(8)] and the chair form of the other six-membered chelate ring [N(10)–C(13)–N(7)–Ni(1)–N(8)–C(15)] formed between the bicyclononane rings and the nickel ion. The six-membered chelate rings (chair forms) are shown in dark grar. Hydrogen atoms have been omitted for clarity.

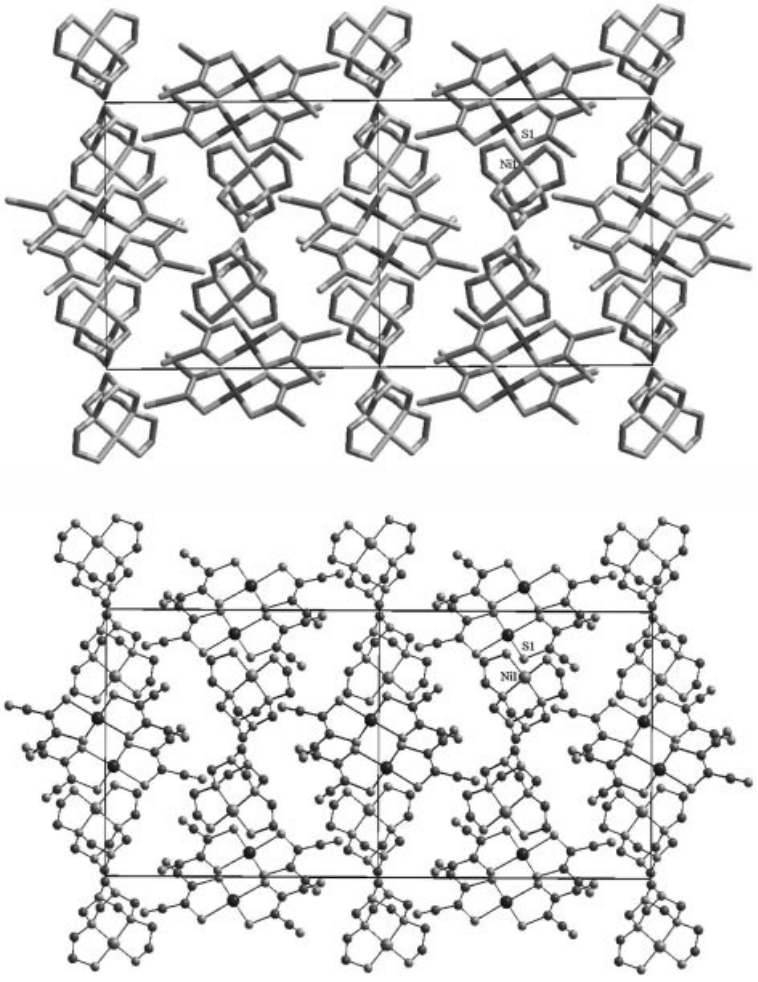

Figure 3. Packing diagram (4×4 cells) of $[Ni(C_9H_{22}N_6)][M(mnt)_2]$ (M = Cu^{2+}, Ni^{2+}, and Pd^{2+}): wire-frame representation (top) and ball-and-stick representation (bottom) showing the mixed-stacked CC–AA–CC–AA-type arrangement along the crystallographic *c* axis (C = cation and A = anion). Hydrogen atoms have been omitted for clarity.

from N(7) and N(8) to their immediate carbon atoms are the longest, with an average distance of 1.507 ± 0.003 Å. This is considerably longer than the average N–C bond lengths (1.445 ± 0.004 Å) observed for the other six bonds from N(9) and N(10) to their immediate carbon atoms. The lengthening of these N–C bonds is consistent with the fact that N(7) and N(8) are coordinated to the nickel ion and N(9) and N(10) are not.

The N(5)–Ni(1)–N(7) bite angle in one of the five-membered chelate rings [Ni(1)–N(5)–C(17)–C(16)–N(7)] in the cation of **1** is 87.45(10)° and the N(6)–Ni(1)–N(8) bite angle of the other five-membered ring [Ni(1)–N(8)–C(10)–C(9)–N(6)] is 87.35(10)°. The respective bite distances are 2.647 and 2.642 Å (Figure 1). These values are consistent with those in the five-membered rings of other Ni^{II} macrocyclic complexes,[16–19] including the tetraazabicyclononane–Ni^{II} complex $[Ni(C_{12}H_{27}N_7)](ClO_4)_2$.[15] The N(5)–Ni(1)–N(6) angle, which is not constrained by any ring closure (Figure 1), is 94.99(11)° and the length between the N(5) and N(6) atoms is 2.817 Å. Interestingly, the N(7)–Ni(1)–N(8) bite angle of 90.11(10)° and the N(7)–N(8) bite distance of 2.713 Å involving two six-membered rings in bicyclononane are considerably smaller than those for the open side of the cation. This N(7)–N(8) separation, in principle, should be determined by the intracyclic valence angles at the C(11), C(15), C(13), C(14), N(9), and N(10) centers of the bicyclononane ring (Figure 1). These angles, which range from 111.7° to 114.6°, are already larger than the normal values of 107° for N(sp^3) and 109.5° for C(sp^3). Therefore, there is no chance for a lengthening of the bite distance between atoms N(7) and N(8).

There are four six-membered and two five-membered rings in the cation. The two six-membered rings [C(12)–N(9)–C(14)–N(7)–C(13)–N(10) and C(12)–N(9)–C(11)–N(8)–C(15)–N(10)] in the bicyclononane ring assume a stable chair conformation with average intracyclic torsion angles of 58° and 57.44° in the cation of compound **1** (see Figure 1). The two six-membered chelate rings formed between the bicyclononane ring and the nickel ion also assume a chair conformation. These rings are Ni(1)–N(7)–C(14)–N(9)–C(11)–N(8) and N(10)–C(13)–N(7)–Ni(1)–N(8)–C(15) in the cation of compounds **1**–**3**, as shown in Figure 2.

The anion $[Cu(mnt)_2]^{2-}$ has a planar structure, in good agreement with other relevant literature data.[20] The anion (A) and the cation (C) are arranged face to face, forming a mixed-stacked CC–AA-CC–AA-type arrangement along the crystallographic *a* axis (Figure 3). The angle between the planes of the cation and anion, defined by Ni(1)–N(5)–N(7)–N(8)–N(6) and Cu(1)–S(1)–S(3)–S(2)–S(4), is 38.28(6)° (Figure 1) for compound **1**, which comes under the category of noncoplanar structures among ion-pair compounds. The closest intra-stack distance of 3.947 Å is found between Ni(1) and S(1) in the case of compound **1** (Figure 3).

The single-crystal X-ray diffraction analyses revealed that compounds **2** and **3** are isostructural with **1** and therefore the unit-cell dimensions, volumes, and other related data for the structure determinations of all three compounds vary only slightly (see table in Experimental Section). Selected bond lengths and angles for compounds **1**–**3** are presented in Table 1.

Table 1. Selected bond lengths [Å] and angles [°] for compounds **1**–**3** (see Figure 1).[a]

Compound **1**			
Ni(1)–N(5)*	1.909(2)	Ni(1)–N(6)*	1.911(2)
Ni(1)–N(7)	1.920(2)	Ni(1)–N(8)	1.914(2)
Cu(1)–S(1)*	2.2574(10)	Cu(1)–S(2)*	2.2624(10)
Cu(1)–S(3)*	2.2766(10)	Cu(1)–S(4)	2.2793(10)
S(1)–C(2)	1.732(3)	N(3)–C(7)	1.137(4)
N(5)*–C(17)	1.476(4)	N(6)*–C(9)	1.477(4)
N(5)–Ni(1)–N(6)	94.99(11)	N(6)–Ni(1)–N(8)	87.35(10)
N(5)–Ni(1)–N(7)	87.45(10)	S(1)–Cu(1)–S(2)	175.21(3)
S(1)–Cu(1)–S(3)	90.74(4)	C(1)–S(3)–Cu(1)	101.86(10)
Compound **2**			
Ni(1)–N(5)*	1.901(2)	Ni(1)–N(6)*	1.905(2)
Ni(1)–N(7)	1.914(2)	Ni(1)–N(8)	1.915(2)
Ni(2)–S(2)*	2.1660(11)	Ni(2)–S(1)*	2.1672(11)
Ni(2)–S(3)*	2.1769(9)	Ni(2)–S(4)	2.1817(9)
S(1)–C(2)	1.734(3)	N(3)–C(7)	1.140(4)
N(5)*–C(17)	1.479(3)	N(6)*–C(9)	1.480(3)
N(5)–Ni(1)–N(6)	95.06(10)	N(5)–Ni(1)–N(7)	87.44(9)
N(6)–Ni(1)–N(7)	176.16(9)	N(6)–Ni(1)–N(8)	87.28(9)
N(7)–Ni(1)–N(8)	90.12(9)	S(1)–Ni(2)–S(3)	92.00(4)
C(1)–S(3)–Ni(2)	103.41(9)	C(6)–S(4)–Ni(2)	102.64(10)
Compound **3**			
Ni(1)–N(6)*	1.903(4)	Ni(1)–N(5)*	1.908(4)
Ni(1)–N(7)	1.909(4)	Ni(1)–N(8)	1.909(4)
Pd(1)–S(2)*	2.2836(15)	Pd(1)–S(1)*	2.2866(15)
Pd(1)–S(3)*	2.2924(12)	Pd(1)–S(4)	2.2955(13)
S(1)–C(2)	1.740(5)	N(3)–C(7)	1.135(6)
N(5)*–C(17)	1.477(6)	N(6)*–C(9)	1.471(6)
N(6)–Ni(1)–N(5)	94.95(16)	N(5)–Ni(1)–N(7)	87.44(16)
N(6)–Ni(1)–N(8)	87.28(16)	N(7)–Ni(1)–N(8)	90.24(15)
S(2)–Pd(1)–S(1)	179.35(4)	S(2)–Pd(1)–S(3)	89.41(4)
C(1)–S(3)–Pd(1)	102.10(16)		

[a] Atoms marked with an asterisk * are involved in N–H···S hydrogen-bonding interactions.

N–H···S Hydrogen Bonds Between the Cation and Anion

The inorganic transition metal complex NiL^{2+} (L = $C_9H_{22}N_6$ = 3,7-bis(2-aminoethyl)-1,3,5,7-tetraazabiclo-[3.3.1]nonane) was chosen as a cation since the nickel-coordinated NH_2 groups can provide potential points of organization for the formation of N–H···S hydrogen bonds with the thiolate sulfur atoms of the anions $[M(mnt)_2]^{2-}$ (M = Cu^{2+}, Ni^{2+}, Pd^{2+}). Even though the electronegativity difference between H and S (δ = 0.38, Pauling scale) is very small compared to those between H and X (X = Cl, N, O), and therefore the hydrogen bonds involving H and S will necessarily be weak due to the poorer match between the hard proton and soft sulfur, N–H···S hydrogen bonds have been observed in crystals of sulfur-containing organic molecules,[21] inorganic coordination complexes,[13,22] and metalloproteins.[10–12] In many cases, N–H···S hydrogen bonds play important roles, for example, the arrangement of proteins having amide and amine functional groups

around Fe–S clusters in *Pasteurella aerogenes* ferredoxin and *Clostridium pasteurianum* rubredoxin has been suggested to contribute to the stabilization of the negatively charged cluster by providing possible hydrogen-bond donors in forming N–H···S hydrogen bonds.[11]

The N–H···S bonds involving the amine nitrogen atoms of the cation $[Ni(C_9H_{22}N_6)]^{2+}$ and the dithiolate sulfur atoms of $[M(mnt)_2]^{2-}$ (M = Cu^{2+}, Ni^{2+}, Pd^{2+}) are illustrated in Figure 4; the geometrical parameters of these hydrogen bonds are presented in Table 2. As shown in Figure 4, the cation interacts with two different anions through three N–H···S hydrogen bonds (two H-bonds with one anion and one H-bond with another anion). Similarly, the anion is hydrogen bonded to two different cations through three hydrogen bonds. This results in the formation of a chain-like arrangement consisting of alternating cations and anions, as shown in Figure 5. The N···S and H···S distances are 3.485–3.512 and 2.65–2.73 Å, respectively, for compound **1**. The same distances in **2** are 3.468–3.527 and 2.63–2.76 Å and in **3** are 3.471–3.500 and 2.64–2.74 Å (see Table 2). The N–H···S bond angles in these compounds range from 142.3° to 159.6° and show a direct correlation whereby a decreasing bond angle results in a lengthening, and therefore weakening, of the hydrogen bond (Table 2). These N–H···S hydrogen-bond parameters are similar to those observed in the crystal structure of *Clostridium pasteurianum* rubredoxin protein.[11]

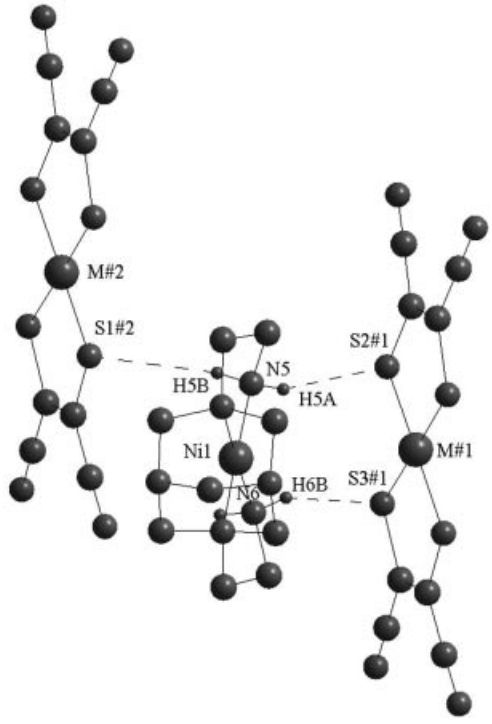

Figure 4. Crystal structure of compounds $[Ni(C_9H_{22}N_6)][M(mnt)_2]$ (M = Cu^{2+}, Ni^{2+}, and Pd^{2+}) showing intermolecular N–H···S hydrogen bonding between the cation and anion. Dotted lines indicate the N–H···S hydrogen bonds. Methylene hydrogen atoms have been omitted for clarity. Atoms with additional labels #1 and #2 are related to each other by the following symmetry operations: #1 1 – *x*, –*y*, 1 – *z*; #2 –*x*, –*y*, 1 – *z*.

Table 2. Hydrogen bonds for compounds **1**–**3** (see Figure 4).[a]

D–H···A	*d*(D···H)	*d*(H···A)	*d*(D···A)	<(DHA)
Compound **1**				
N5–H5A···S2 #1	0.90	2.65	3.499(3)	158.3
N5–H5B···S1 #2	0.90	2.73	3.485(3)	142.3
N6–H6B···S3 #1	0.90	2.68	3.512(3)	155.0
Compound **2**				
N5–H5A···S2 #1	0.90	2.66	3.520(3)	159.6
N5–H5B···S1 #2	0.90	2.76	3.527(3)	144.1
N6–H6B···S3 #1	0.90	2.63	3.468(3)	156.0
Compound **3**				
N5–H5A···S2 #1	0.90	2.65	3.499(5)	157.5
N5–H5B···S1#2	0.90	2.74	3.500(5)	142.8
N6–H6B···S3 #1	0.90	2.64	3.471(5)	154.3

[a] Atoms with additional labels #1 and #2 are related to each other by symmetry operations: #1 1 –*x*, –*y*, 1 – *z*; #2 –*x*, –*y*, 1 – *z*.

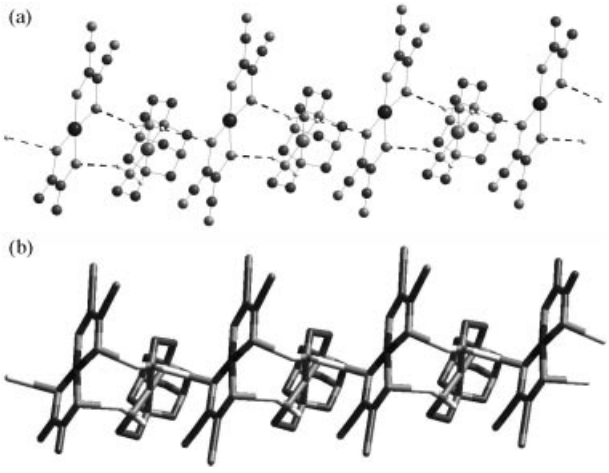

Figure 5. Chain-like arrangement consisting of alternating $[Ni(C_9H_{22}N_6)]^{2+}$ (cation) and $[M(mnt)_2]^{2-}$ (anion) formed by N–H···S hydrogen bonds in the crystal structure of $[Ni(C_9H_{22}N_6)][M(mnt)_2]$ (M = Cu^{2+}, Ni^{2+}, and Pd^{2+}): (a) ball-and-stick representation and (b) wire-frame representation. Methylene hydrogen atoms have been omitted for clarity.

The average Cu–S_H bond length in **1** involving hydrogen-bonded sulfur (S_H) is 2.265(1) Å, which is 0.014 Å shorter than the Cu–S_N bond length [2.279(1) Å], in which S_N is not involved in hydrogen-bonding interactions. In the case of compound **2**, the average Ni–S_H bond length [2.170(1) Å] is 0.012 Å shorter than the Ni–S_N bond length [2.182(1) Å]. Compound **3** also follows the same trend but with a smaller difference [average Pd–S_H = 2.287(1) and Pd–S_N = 2.295(1) Å]. The shortening of the M–S_H (M = Cu^{2+}, Ni^{2+}, Pd^{2+}) bonds compared to the M–S_N bond can be explained by a molecular orbitals approach. Thiolate sulfurs are σ- and π-electron donors and the π orbitals that are occupied by a lone pair of electrons interact with the occupied p and d orbitals on the metal ion M^{2+}. The occupation of these metal orbitals, which have antibonding character, results in the weakening of the M–S interaction.[23] However, in the present case, it can be expected that the N–H···S hydrogen bonding stabilizes the sulfur π-donor orbitals and thereby diminishes the M–S antibonding interaction. This results in

a slight shortening of the M–S_H (M = Cu^{2+}, Ni^{2+}, Pd^{2+}) bonds compared to the M–S_N bonds.

In concert with the metal–sulfur bond length changes in the anion $[M(mnt)_2]^{2-}$, it is expected that the N–H bonds would be lengthened by the N–H···S hydrogen-bonding interaction, while the C–N_H and Ni–N_H bonds (N_H = hydrogen-bonded nitrogen) in the cation $[Ni(C_9H_{22}N_6)]^{2+}$ would be shortened.[24,25] In the present study, the N–H bond lengths cannot be considered because the amine hydrogens were assigned positions on the basis of geometrical considerations in the crystal-structure determination. On the other hand, and in contrast to our expectations, a trend of increasing C–N_H and Ni–N_H bond lengths in the $[Ni(C_9H_{22}N_6)]^{2+}$ cations of **1**, **2**, and **3** is evident when comparing them with those in the crystal structure of $[Ni(C_9H_{22}N_6)](ClO_4)_2$. The average C–N and Ni–N bond lengths (adjacent to amine groups) in $[Ni(C_9H_{22}N_6)](ClO_4)_2$ are 1.37(5) and 1.90(3) Å, respectively.[15] The corresponding average C–N_H and Ni–N_H distances in the cations of **1**–**3** are 1.476(4) and 1.910(2) Å for **1**, 1.479(2) and 1.903(2) Å for **2**, and 1.474(6) and 1.905(2) Å for **3**. The shortening of the Ni–N_H bond lengths compared to the Ni–N_N (N_N = non-hydrogen-bonded nitrogen) bond lengths in the cations of **1**–**3** [average Ni–N_N bond lengths are 1.917(2), 1.914(2), and 1.909(4) Å for **1**–**3**, respectively] is consistent with the fact that the N_H atoms are involved in N–H···S hydrogen-bonding interactions.

IR Spectra

The N–H···S hydrogen-bonding interactions described above are also reflected in the IR spectra of compounds **1**–**3**. The perchlorate salt of the cation, $[Ni(C_9H_{22}N_6)](ClO_4)_2$ exhibits two NH bands at 3342 and 3296 cm^{-1} in its IR spectrum (Figure 6, a). In the IR spectra of compounds **1**–**3** these bands shift to about 3260 and 3200 cm^{-1}, respectively (Figure 6, b–d). This large shift of the NH bands suggests that compounds **1**–**3** have intermolecular N–H···S hydrogen bonds involving cation and anion. The CN bands of the anions $[M(mnt)_2]^{2-}$ (M = Cu^{2+}, Ni^{2+}, Pd^{2+}) in compounds **1**–**3** appear at around 2195 cm^{-1} and the corresponding C=C bands are observed at 1465, 1485, and 1485 cm^{-1}, respectively, for **1**–**3** (for IR spectra, see Supporting Information).

^{1}H NMR Spectra

The ^{1}H NMR spectra of $[Ni(C_9H_{22}N_6)](ClO_4)_2$ and compound **2** were recorded in [D_6]DMSO (see SI-Figure 6 in the Supporting Information). The protons of the two NH_2 groups are observed at δ = 5.75 and 6.97 ppm, respectively, in the spectrum of $[Ni(C_9H_{22}N_6)](ClO_4)_2$. These two peaks are shifted downfield, appearing at δ = 7.18 and 8.42 ppm, respectively, in the spectrum of **2**, which also shows the CH_2 protons in the range δ = 2 to 6 ppm. The downfield shift of the NH_2 protons from $[Ni(C_9H_{22}N_6)](ClO_4)_2$ to **2** can be ascribed to the existence of the N–H···S hydrogen-bonding

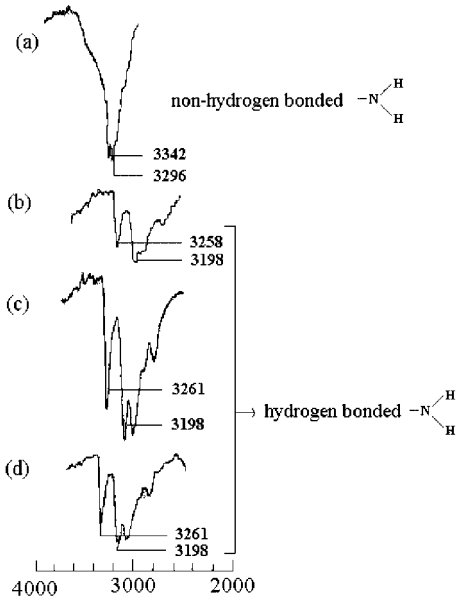

Figure 6. Selected IR bands in the NH_2 region of (a) $[Ni(C_9H_{22}N_6)](ClO_4)_2$, (b) $[Ni(C_9H_{22}N_6)][Cu(mnt)_2]$ (**1**), (c) $[Ni(C_9H_{22}N_6)][Ni(mnt)_2]$ (**2**), and (d) $[Ni(C_9H_{22}N_6)][Pd(mnt)_2]$ (**3**) in the solid state (KBr pellets).

interactions between cation and anion (hydrogen bonding decreases the electron density around proton). A similar downfield shift of the amide NH signal was observed in the ^{1}H NMR spectrum of the compound $(NEt_4)_2[Hg(S\text{-}2\text{-}CH_3NHCOC_6H_4)_4]$ compared with the bis(carbamoylthiophenoate) complex in [D_6]DMSO due to the formation of intramolecular N–H···S hydrogen bonds in the mercury complex.[26]

When the initial concentration of **2** is increased a steady chemical-shift change is observed for the NH_2 protons involved in N–H···S hydrogen-bonding interactions. This demonstrates that the percentage of hydrogen-bonded species increases with increasing initial concentrations of **2**. At a concentration of 1×10^{-3} M no shift of the NH_2 protons with respect to that of $[Ni(C_9H_{22}N_6)](ClO_4)_2$ was observed. However, at higher concentrations (in the range of 0.013 to 0.034 M) a downfield shift of the NH_2 protons from $[Ni(C_9H_{22}N_6)](ClO_4)_2$ to **2** was observed (see Figure 7 in the Supporting Information for concentration-dependent NMR spectra). The ^{1}H NMR spectra of $[Ni(C_9H_{22}N_6)](ClO_4)_2$ were recorded in the same concentration range used for compound **2**; the peak positions for the NH_2 group remained essentially same.

Electrochemistry

The cationic complex $[Ni(C_9H_{22}N_6)](ClO_4)_2$ shows a quasi-reversible oxidation at +1.24 V vs. SCE and a quasi-reversible reduction at –1.34 V vs. SCE in MeCN solution.[15] However, its ion-pair compounds **1**–**3** are not soluble in MeCN, therefore we performed the electrochemical studies in DMF. In DMF, the reversible oxidation and reduction are observed at +1.00 V vs. SCE and at –1.30 V vs.

SCE, respectively, for $[Ni(C_9H_{22}N_6)](ClO_4)_2$ (see Supporting Information). Cyclic voltammograms of **1**–**3** are shown in Figure 7. Compounds **2** and **3** show similar features in their cyclic voltammograms. The reversible reductions at around –1.30 V (vs. SCE) for $[Ni(C_9H_{22}N_6)](ClO_4)_2$ become quasi-reversible in its ion-pair compounds and the oxidative response at around +1.00 V (vs. SCE) for $[Ni(C_9H_{22}N_6)](ClO_4)_2$ is not clearly observed in the ion-pair compounds. Instead, all three cyclic voltammograms (Figure 7) exhibit a strong irreversible oxidation at around +1.16 V (vs. SCE) whose shape is rather complicated. This can be assigned to the oxidation of the dithiolate sulfurs of the mnt ligands (by comparing the cyclic voltammograms of $[Bu_4N]_2[M(mnt)_2]$). This complicated feature might also include the oxidative response of $[Ni(C_9H_{22}N_6)]^{2+}$ at a shifted (higher) potential, which is in agreement with the small bump observed around +1.25 V for all complexes. These data indicate that the oxidation of $[Ni(C_9H_{22}N_6)]^{2+}$ becomes somewhat more difficult in the ion-pair compounds **1**–**3** than in the perchlorate complex $[Ni(C_9H_{22}N_6)](ClO_4)_2$ and the reduced complex $[Ni(C_9H_{22}N_6)]^{+}$ becomes more unstable in the ion-pair compounds than in the perchlorate complex (on the cyclic voltammetric timescale). This implies that the stability of $[Ni(C_9H_{22}N_6)]^{2+}$ in its ion-pair compounds would make the transition from Ni^{II} to Ni^{III} or Ni^{I} more unfavorable than in its perchlorate salt. Compound **1** shows an additional irreversible reduction at around –0.75 V vs. SCE (Figure 7, a) that is not observed in the case of compounds **2** and **3** (Figures 7, parts b and c, respectively). We assign this reductive response to the $[Cu(mnt)_2]^{2-}/[Cu(mnt)_2]^{3-}$ couple based on relevant literature data.[27] Compounds **1**–**3** exhibit a reversible oxidation that corresponds to the couple $[M(mnt)_2]^{-}/[M(mnt)_2]^{2-}$ (M = Cu^{2+}, Ni^{2+} and Pd^{2+}; 0.33 V vs. SCE for **1**, 0.33 V vs. SCE for **2** and 0.54 V vs. SCE for **3** in DMF).

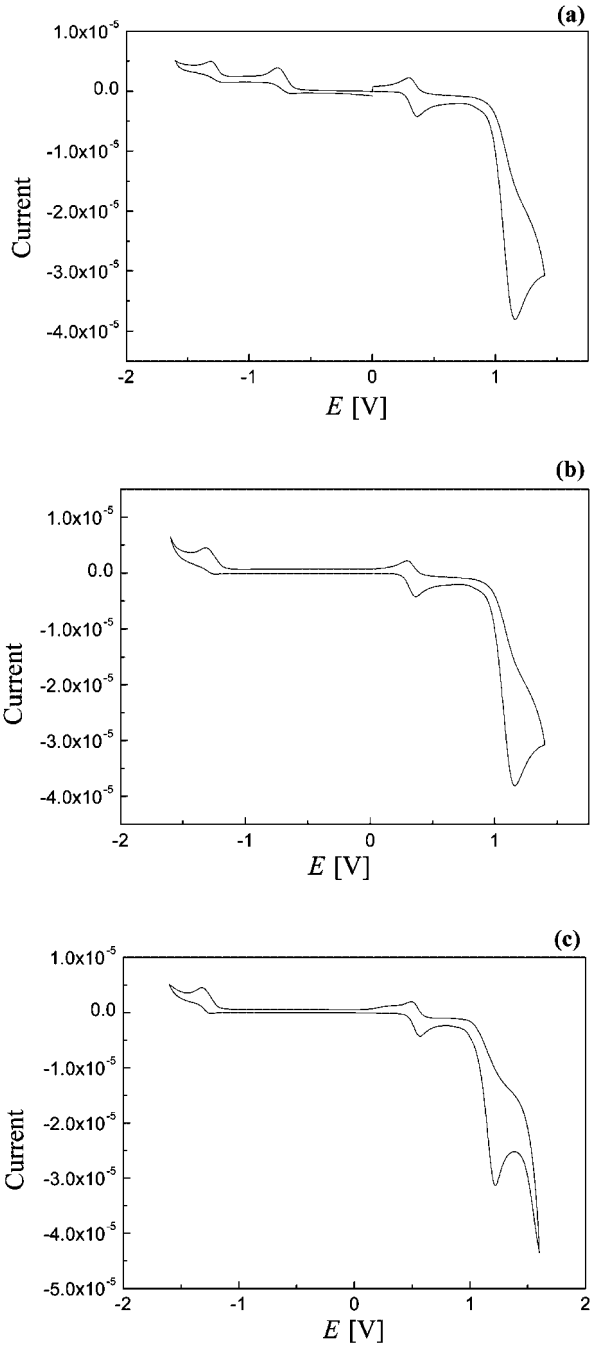

Figure 7. Cyclic voltammograms of a 1.0 mM solution of (a) $[Ni(C_9H_{22}N_6)][Cu(mnt)_2]$ (**1**), (b) $[Ni(C_9H_{22}N_6)][Ni(mnt)_2]$ (**2**), and (c) $[Ni(C_9H_{22}N_6)][Pd(mnt)_2]$ (**3**) in DMF at room temperature. Scan rate: 100 mV s^{-1}. Current given in A.

UV/Vis-NIR Spectra

The UV/Vis spectra of compounds **1**–**3** were measured both in solution and the solid state at room temperature. The perchlorate salt of the cation $[Ni(C_9H_{22}N_6)](ClO_4)_2$ exhibits a d-d band at around 450 nm in the solid state and at 440 nm in solution (ε = 80 $M^{-1}cm^{-1}$ in MeCN), which is the characteristic absorption for a square-planar Ni^{II}-N_4 chromophore (Figures 18 and 19 in the Supporting Information). The d-d band of $[Ni(C_9H_{22}N_6)]^{2+}$ at 440 nm is obscured by the intense MLCT charge-transfer bands for the metal–dithiolene moieties in the ion-pair complexes (at around 430 nm for **1**, 470 nm for **2**, and 430 nm for **3**). The d-d bands at around 1100 (for **1**), 860 (for **2**), and 630 nm (for **3**) are characteristic features of $[Cu(mnt)_2]^{2-}$, $[Ni(mnt)_2]^{2-}$, and $[Pd(mnt)_2]^{2-}$ respectively (see SI-Figure 20 in the Supporting Information).

ESR Spectroscopy

The ESR spectrum of compound **1** in DMF at liquid-nitrogen temperature was also measured. It exhibits hyperfine structure due to $^{63,65}Cu$ nuclei. Interestingly, both $g_{\|}$ and $g_{\perp}$ features are resolved due to $^{63,65}Cu$ hyperfine coupling, which is very rarely observed in metal–dithiolene complexes. The average value of the hyperfine coupling parameters (determined from $|A_{\|}|$ = 15.3 mT and $|A_{\perp}|$ = 4.8 mT) is 8.3 mT, which is not identical to that (7.4 mT) of the solution ESR spectrum at room temperature (see SI-Figures

21–23 in the Supporting Information). This is consistent with the NMR studies.

Conclusion

Numerous model compounds of sulfur-containing metallo-proteins have been reported that emphasize the importance of N–H···S hydrogen bonds in stabilizing the negatively charged metal–sulfur cluster (the active site) of the relevant protein. Intramolecular N–H···S hydrogen bonding was observed in many of these model studies and, in a few cases, intermolecular hydrogen bonding was also identified. We have introduced, for the first time, this N–H···S hydrogen-bonding interaction between a novel cationic inorganic complex $[Ni(C_9H_{22}N_6)]^{2+}$ (that has H-bond donor sites) and the classical inorganic anionic complexes $[M(mnt)_2]^{2-}$ ($M = Cu^{2+}$, Ni^{2+} and Pd^{2+}) with dithiolato sulfur anions as H-bond acceptor sites. The existence of such supramolecular intermolecular N–H···S interactions in this new family of ion-pair compounds is additionally supported by IR, ^1H NMR, and ESR spectral studies. The complex cation $[Ni(C_9H_{22}N_6)]^{2+}$ was reported earlier as its perchlorate salt, although its crystal structure was not discussed in detail because of disorder problems. We have succeeded in resolving this disorder problem in the crystal structures of the ion-pair compounds **1**–**3**.

Experimental Section

General: Microanalytical (C, H, N, S) data were obtained with a FLASH EA 1112 Series CHNS Analyzer. IR spectra were recorded for KBr pellets with a JASCO FT/IR-5300 spectrometer in the region 400–4000 cm^{-1}. Electronic spectra were recorded with a UV-3101PC/UV/Vis-NIR spectrophotometer (Shimadzu) equipped with a diffuse reflectance accessory (reflectance spectra were recorded for KBr pellets). The diffuse reflectance spectra obtained were then Kubelka–Munk corrected. The ESR spectra were recorded with a (JEOL) JES-FA200 ESR spectrometer. A Cypress model CS-1090/CS-1087 electroanalytical system was used for cyclic voltammetric experiments. The electrochemical experiments were measured in DMF containing Bu_4NClO_4 as a supporting electrolyte, using a conventional cell consisting of two platinum wires as working and counter electrodes, and a saturated calomel electrode (SCE) as reference. The potentials reported here are uncorrected for junction contributions. Some electrochemical measurements were performed on a BAS i Epsilon-EC Bioanalytical System Inc. using Ag/AgCl reference electrode and glassy carbon as a working electrode. Powder X-ray diffraction data were collected on Phillips PW 3710 diffractometer. EDAX analyses were performed using Philips XL 30 SEM equipment.

Materials: All commercially available chemicals were of reagent grade and were used as received without further purification. The solvents were dried and distilled according to standard procedures for the electrochemical and spectroscopy experiments. The acyclic Ni^{II} complex of 3,7-bis(2-aminoethyl)-1,3,5,7-tetraazabiclo[3.3.1]-nonane was synthesized as its perchlorate salt according to a reported method.[15] The salts $[Bu_4N]_2[M(mnt)_2]$ ($M = Ni^{2+}$, Pd^{2+}, and Cu^{2+}) were prepared according to a literature procedure.[28] Disodium maleonitriledithiolate [the disodium salt of 1,2-dicyanoethylenedithiolate (Na_2mnt)] was prepared following a synthetic procedure described in the same paper.[28]

Synthesis of $[Ni(C_9H_{22}N_6)][Cu(mnt)_2]$ (1): $[Ni(C_9H_{22}N_6)](ClO_4)_2$ (0.047 g, 0.10 mmol) was dissolved in 10 mL of MeCN by mild heating in a water bath. The resulting clear, yellow solution was treated with $[Bu_4N]_2[Cu(mnt)_2]$ (0.082 g, 0.1 mmol) dissolved in 15 mL of MeCN. The final reaction mixture was then heated to about 50 °C in an oil bath for 10 min with stirring, whereby the dark microcrystalline compound **1** precipitated out within a day. The crystals of **1** were filtered, washed with diethyl ether, and dried at room temperature. Yield: 0.045 g (74% based on Cu). $C_{17}H_{22}CuN_{10}NiS_4$ (616.94): calcd. C 33.09, H 3.59, N 22.70, S 20.79; found C 33.29, H 3.48, N 22.59, S 21.01. IR (KBr): $\tilde{\nu}$ = 3258 (w), 3192 (m), 2191 (s), 1570 (w), 1464 (s), 1281 (w), 1150 (m), 1086 (s), 992 (w), 941 (m), 908 (w), 856 (s), 814 (s), 716 (w), 607 (m), 586 (w), 511 (s) cm^{-1}. UV/Vis/NIR (DMF): λ_{max} (ε) = 321 nm (36360 $M^{-1}cm^{-1}$), 372 (23230), 426 (12120), 485 (10100), 1200 (74).

Single crystals suitable for an X-ray structure determination were grown in a λ-shaped glass tube with two terminals. $[Ni(C_9H_{22}N_6)](ClO_4)_2$ was dissolved in 10 mL of MeCN in a 20-mL round-bottomed flask and this was fixed to one terminal of the tube; the other terminal of the tube was connected to a 20-mL round-bottomed flask containing 10 mL of an MeCN solution of $[Bu_4N]_2[Cu(mnt)_2]$. Finally, the empty part of the tube was slowly filled with MeCN (from the top) and sealed. The crystals collected after 25 days from the top of the tube were identified as **1**.

Synthesis of $[Ni(C_9H_{22}N_6)][Ni(mnt)_2]$ (2): This compound was synthesized by stirring an MeCN solution (10 mL) of $[Ni(C_9H_{22}N_6)](ClO_4)_2$ (0.047 g, 0.10 mmol) with an MeCN solution (15 mL) of $[Bu_4N]_2[Ni(mnt)_2]$ (0.082 g, 0.1 mmol) at room temperature for half an hour. The red microcrystals of **2** were separated by filtration, washed with diethyl ether, and dried at room temperature. Yield: 0.05 g (82% based on Ni). $C_{17}H_{22}N_{10}Ni_2S_4$ (612.11): calcd. C 33.36, H 3.62, N 22.88, S 20.95; found C 33.58, H 3.53, N 22.78, S 21.06. IR (KBr): $\tilde{\nu}$ = 3264 (w), 3196 (m), 2195 (s), 1570 (w), 1485 (s), 1280 (w), 1233 (m), 1149 (s), 1086 (s), 1055 (m), 990 (m), 943 (w), 909 (w), 856 (s), 814 (s), 713 (w), 605 (s), 546 (w), 509 (s) cm^{-1}. UV/Vis/NIR (DMF): λ_{max} (ε) = 317 nm (41410 $M^{-1}cm^{-1}$), 387 (10100), 482 (6060), 510 (3131), 770 (53).

Single crystals suitable for an X-ray crystal structure determination were grown as described for compound **1**.

Synthesis of $[Ni(C_9H_{22}N_6)][Pd(mnt)_2]$ (3): This compound was synthesized by the same procedure as described for compound **2**, starting from MeCN solutions of $[Ni(C_9H_{22}N_6)](ClO_4)_2$ (0.047 g, 0.1 mmol) and $[Bu_4N]_2[Pd(mnt)_2]$ (0.087 g, 0.1 mmol). Yield: 0.041 g (63% based on Pd). $C_{17}H_{22}N_{10}NiPdS_4$ (659.80): calcd. C 30.94, H 3.36, N 21.23, S 19.44; found C 31.06, H 3.31, N 21.34, S 19.66. IR (KBr): $\tilde{\nu}$ = 3262 (w), 3198 (m), 2195 (s), 1568 (w), 1485 (s), 1338 (m), 1279 (w), 1232 (w), 1202 (w), 1178 (w), 1146 (s), 1086 (s), 1043 (w), 990 (w), 943 (w), 909 (w), 854 (s), 815 (s), 713 (w), 605 (m), 507 (s) cm^{-1}. UV/Vis (DMF): λ_{max} (ε) = 367 nm (2121 $M^{-1}cm^{-1}$), 429 (5050), 450 (5454), 637 (110).

Caution! *Perchlorate salts are potentially explosive and should be handled in small quantities with caution.*

X-ray Crystallography: Crystal data were collected with an Enraf–Nonius CAD4 diffractometer at 25 °C equipped with a graphite-monochromated Mo-K_α (λ = 0.71073 Å) radiation source. An empirical absorption correction based on a series of ψ scans was applied. The structures were solved by direct methods (SHELXS-97)[29] and refined by full-matrix least-squares on F^2 (SHELXL-97).[30] All non-hydrogen atoms were refined anisotropi-

Table 3. Crystal data and structural refinement for compounds **1**, **2** and **3**.

	1	**2**	**3**
Empirical formula	$C_{17}H_{22}CuN_{10}NiS_4$	$C_{17}H_{22}N_{10}Ni_2S_4$	$C_{17}H_{22}N_{10}NiPdS_4$
Formula weight	616.94	612.11	659.80
T [K]	298(2)	298(2)	298(2)
λ [Å]	0.71073	0.71073	0.71073 A
Crystal system	monoclinic	monoclinic	monoclinic
Space group	$P2_1/n$	$P2_1/n$	$P2_1/n$
a [Å]	8.493(2)	8.481(5)	8.489(8)
b [Å]	16.897(5)	16.753(4)	16.904(3)
c [Å]	16.863(8)	16.857(8)	16.898(4)
β [°]	101.77(3)	101.27(4)	101.68(4)
V [Å^3]	2369.1(14)	2348.9(19)	2374(2)
Z	4	4	4
$D_{calcd.}$ [Mg m^{-3}]	1.730	1.731	1.846
μ [mm^{-1}]	2.074	1.988	1.931
F[000]	1260	1256	1328
Crystal size [mm^3]	0.68 × 0.64 × 0.48	0.68 × 0.60 × 0.56	0.68 × 0.36 × 0.32
θ range for Data collection [°]	1.72 to 27.47	1.73 to 27.46	1.72 to 24.97
Reflections collected/unique	5409/5409	5363/5363	4178/4178
Refinement method	Full-matrix least-squares on F^2		
Data/restraints /parameters	5409/0/298	5363/0/298	4178/0/298
Goodness-of-fit on F^2	1.132	1.132	1.291
R_1/wR_2 [$I > 2\sigma(I)$]	0.0306/0.0816	0.0306/0.0790	0.0322/0.1054
R_1/wR_2 (all data)	0.0437/0.0986	0.0463/0.0915	0.0459/0.1110
Largest diff. Peak/hole [e·Å^3]	1.031/–0.417	0.608/–0.503	1.239/–0.465

cally. Hydrogen atoms were introduced at calculated positions and included in the refinement as riding on their respective parent atoms. The crystallographic data and the parameters of structure refinement for compounds **1**–**3** are summarized in Table 3.
CCDC-273272 (for **1**), -273273 (for **2**), and -273274 (for **3**) contain the supplementary crystallographic data for this paper. These data can be obtained free of charge from The Cambridge Crystallographic Data Center via www.ccdc.cam.ac.uk/data_request/cif.

Supporting Information available (for details see the footnote on the first page of this article): Figures related to crystal structures for compounds **1**, **2** and **3**; ^{1}H NMR spectrum for compound **2** and ^{1}H NMR spectra for concentration-dependent NMR studies; IR spectra for compounds **1**, **2** and **3**; cyclic voltammograms for compounds **1**, **2** and **3**; solution and solid-state electronic spectra for compounds **1**, **2** and **3**; ESR spectra for compound **1**; X-ray powder diffraction patterns (simulated and observed).

Acknowledgments

We thank CSIR, Government of India, for financial support [Project No.: 01(1737)/02/EMR-II]. The National X-ray Diffractometer facility at University of Hyderabad by the Department of Science and Technology, Government of India, is gratefully acknowledged. We are grateful to UGC, New Delhi, for providing infrastructure facility at University of Hyderabad under UPE grant. The authors thank Professor S. Pal for providing electrochemical data for this work. We also thank Professor Sabyasachi Sarkar and Mr. Kuntal Pal (Department of Chemistry, IIT Kanpur, India) for helping us by providing some electrochemical data at the revision stage of this work. V. M. thanks CSIR, New Delhi, for a fellowship.

[1] V. Balzani, F. Scandola, *Supramolecular Photochemistry*, Horwood, Chichester, **1991**.
[2] U. T. Mueller-Westerhoff, B. Vance, D. I. Yoon, *Tetrahedron* **1991**, *47*, 909–932.
[3] H. Tanaka, Y. Okano, H. Kobayashi, W. Suzuki, A. Kobayashi, *Science* **2001**, *291*, 285–287.
[4] A. T. Coomber, D. Beljonne, R. H. Friend, J. K. Bredas, A. Charlton, N. Robertson, A. E. Underhill, M. Kurmoo, P. Day, *Nature* **1996**, *380*, 144–146.
[5] C.-T. Chen, S.-Y. Liao, K.-J. Lin, L.-L. Lai, *Adv. Mater.* **1998**, *3*, 334–338.
[6] a) I. Nunn, B. Eisen, R. Benedix, H. Kisch, *Inorg. Chem.* **1994**, *33*, 5079–5085; b) C. Handrosch, R. Dinnebier, G. Bondarenko, E. Bothe, F. Heinemann, H. Kisch, *Eur. J. Inorg. Chem.* **1999**, 1259–1269; c) G. Schmauch, F. Knoch, H. Kisch, *Chem. Ber.* **1994**, *127*, 287–294; d) W. Dümler, H. Kisch, *New J. Chem.* **1991**, *15*, 649–656; e) H. Kisch, B. Eisen, R. Dinnebier, K. Shankland, W. I. F. David, F. Knoch, *Chem. Eur. J.* **2001**, *7*, 738–748.
[7] R. C. Wheland, *J. Am. Chem. Soc.* **1976**, *98*, 3926–3930.
[8] a) H. Kisch, *Coord. Chem. Rev.* **1997**, *159*, 385–396; b) A. Vogler, H. Kunkely, *J. Chem. Soc. Chem. Commun.* **1986**, 1616–1617; c) G. Schmauch, T. Chihara, K. Wakatsuki, M. Hagiwara, H. Kisch, *Bull. Chem. Soc. Jpn.* **1996**, *69*, 2573–2579; d) F. Bigoli, P. Deplano, M. L. Mercuri, M. A. Pellinghelli, L. Pilia, G. Pintus, A. Serpe, E. F. Trogu, *Inorg. Chem.* **2002**, *41*, 5241–5248.
[9] V. Madhu, S. K. Das, *Polyhedron* **2004**, *23*, 1235–1242.
[10] E. T. Adman, *Biochim. Biophys. Acta* **1979**, *549*, 107–144.
[11] E. Adman, K. D. Watenpaugh, L. H. Jensen, *Proc. Natl. Acad. Sci. U. S. A* **1975**, *72*, 4854–4858.
[12] A. Nakamura, N. Ueyama, in *Metal Clusters in Proteins* (Ed.: L. Que), American Chemical Society, Washington, DC, **1998**, chapter 14.
[13] a) N. Ueyama, T. Okamura, A. Nakamura, *J. Am. Chem. Soc.* **1992**, *114*, 8129–8137; b) N. Ueyama, T. Okamura, A. Nakamura, *J. Chem. Soc. Chem. Commun.* **1992**, 1019–1020; c) T. Okamura, N. Ueyama, A. Nakamura, E. W. Ainscough, A. M. Brodie, J. M. Waters, *J. Chem. Soc. Chem. Commun.* **1993**, 1658–1660; d) N. Ueyama, N. Nishikawa, Y. Yamada, T. Oka-

mura, A. Nakamura, *J. Am. Chem. Soc.* **1996**, *118*, 12826–12827; e) N. Ueyama, Y. Yamada, T. Okamura, S. Kimura, A. Nakamura, *Inorg. Chem.* **1996**, *35*, 6473–6484; f) T. Okamura, S. Takamizawa, N. Ueyama, A. Nakamura, *Inorg. Chem.* **1998**, *37*, 18–28; g) N. Ueyama, N. Nishikawa, Y. Yamada, T. Okamura, S. Oka, H. Sakurai, A. Nakamura, *Inorg. Chem.* **1998**, *37*, 2415–2421; h) M. A. Walters, C. L. Roche, A. L. Rheingold, S. W. Kassel, *Inorg. Chem.* **2005**, *44*, 3777–3779; i) M. Kato, T. Okamura, H. Yamamoto, N. Ueyama, *Inorg. Chem.* **2005**, *44*, 1966–1972.

[14] M. A. Walters, J. C. Dewan, C. Min, S. Pinto, *Inorg. Chem.* **1991**, *30*, 2656–2662.

[15] M. P. Suh, W. Shin, H. Kim, C. H. Koo, *Inorg. Chem.* **1987**, *26*, 1846–1852.

[16] T. Ito, K. Toriumi, *Acta Crystallogr. Sect. B* **1981**, *37*, 88–92.

[17] R. Murray-Rust, J. Murray-Rust, *Acta Crystallogr. Sect. B* **1979**, *35*, 1704–1706.

[18] G. Ferguson, R. J. Restivo, R. W. Hay, *Acta Crystallogr. Sect. B* **1979**, *35*, 159–162.

[19] M. F. Bailey, I. E. Maxwell, *J. Chem. Soc., Dalton Trans.* **1972**, 938–944.

[20] a) P. Kuppusamy, B. L. Ramakrishna, P. T. Manoharan, *Inorg. Chem.* **1984**, *23*, 3886–3892; b) S. S. Staniland, W. Fujita, Y. Umezono, K. Awaga, P. J. Camp, S. J. Clark, N. Robertson, *Inorg. Chem.* **2005**, *44*, 546–551.

[21] a) M. K. Krepps, S. Parkin, D. A. Atwood, *Cryst. Growth Des.* **2001**, *1*, 291–297; b) K. C. Kumara Swamy, S. Kumara Swamy, S. Raja, K. S. Kumar, *J. Chem. Crystallogr.* **2001**, *31*, 51–56.

[22] a) N. Ueyama, K. Taniuchi, T. Okamura, T. Nakamura, H. Maeda, S. Emura, *Inorg. Chem.* **1996**, *35*, 1945–1951; b) B. R. Srinivasan, S. N. Dhuri, C. Näther, W. Bensch, *Acta Crystallogr., Sect. E* **2002**, *58*, m622–m624; c) B. R. Srinivasan, S. N. Dhuri, C. Näther, W. Bensch, *Acta Crystallogr. Sect. C* **2003**, *59*, m124–m127; d) B. R. Srinivasan, M. Poisot, C. Näther, W. Bensch, *Acta Crystallogr., Sect. E* **2004**, *60*, i136–i138; e) B. R. Srinivasan, S. N. Dhuri, M. Poisot, C. Näther, W. Z. Bensch, *Naturforsch., Teil B* **2004**, *59*, 1083–1092; f) B. R. Srinivasan, S. N. Dhuri, M. Poisot, C. Näther, W. Bensch, *Z. Anorg. Allg. Chem.* **2005**, *631*, 1087–1094.

[23] S. Harris, *Polyhedron* **1989**, *8*, 2843–2882.

[24] V. Gutmann, G. Resch, W. Linert, *Coord. Chem. Rev.* **1982**, *43*, 133–164 and references cited therein.

[25] M. Kitano, K. Kuchitsu, *Bull. Chem. Soc. Jpn.* **1973**, *46*, 3048–3051.

[26] M. Kato, K. Kojima, T. Okamura, H. Yamamoto, T. Yamamura, N. Ueyama, *Inorg. Chem.* **2005**, *44*, 4037–4044.

[27] S. P. Best, S. A. Ciniawsky, R. J. H. Clark, R. C. S. McQueen, *J. Chem. Soc. Dalton Trans.* **1993**, 2267–2271.

[28] A. Davison, R. H. Holm, *Inorg. Synth.* **1967**, *10*, 8–26.

[29] G. M. Sheldrick, *SHELXS-97*, *A Program for Structure Solution*, University of Göttingen, Göttingen, Germany, **1997**.

[30] G. M. Sheldrick, *SHELXL-97*, *A Program for Structure Refinement*, University of Göttingen: Göttingen, Germany, **1997**.

Received: August 26, 2005
Published Online: February 15, 2006

